Cancer Therapy: Preclinical

Clinical Cancer Research

Combination Small Molecule MEK and PI3K Inhibition Enhances Uveal Melanoma Cell Death in a Mutant *GNAQ*- and *GNA11*-Dependent Manner

Jahan S. Khalili[1,2], Xiaoxing Yu[1,2], Ji Wang[1,2], Brendan C. Hayes[1], Michael A. Davies[1,2], Gregory Lizee[1], Bita Esmaeli[3], and Scott E. Woodman[1,2]

Abstract

Purpose: Activating Q209L/P mutations in *GNAQ* or *GNA11* (*GNAQ/11*) are present in approximately 80% of uveal melanomas. Mutant *GNAQ/11* are not currently therapeutically targetable. Inhibiting key downstream effectors of GNAQ/11 represents a rational therapeutic approach for uveal melanomas that harbor these mutations. The mitogen-activated protein/extracellular signal–regulated kinase/mitogen-activated protein kinase (MEK/MAPK) and PI3K/AKT pathways are activated in uveal melanoma. In this study, we test the effect of the clinically relevant small molecule inhibitors GSK1120212 (MEK inhibitor) and GSK2126458 (pan class I PI3K inhibitor) on uveal melanoma cells with different *GNAQ/11* mutation backgrounds.

Experimental Design: We use the largest set of genetically annotated uveal melanoma cell lines to date to carry out *in vitro* cellular signaling, cell-cycle regulation, growth, and apoptosis analyses. RNA interference and small molecule MEK and/or PI3K inhibitor treatment were used to determine the dependency of uveal melanoma cells with different *GNAQ/11* mutation backgrounds on MEK/MAPK and/or PI3K/AKT signaling. Proteomic network analysis was done to unveil signaling alterations in response to MEK and/or PI3K small molecule inhibition.

Results: *GNAQ/11* mutation status was not a determinant of whether cells would undergo cell-cycle arrest or growth inhibition to MEK and/or phosphoinositide 3-kinase (PI3K) inhibition. A reverse correlation was observed between MAPK and AKT phosphorylation after MEK or PI3K inhibition, respectively. Neither MEK nor PI3K inhibition alone was sufficient to induce apoptosis in the majority of cell lines; however, the combination of MEK + PI3K inhibitor treatment resulted in the marked induction of apoptosis in a *GNAQ/11* mutant–dependent manner.

Conclusions: MEK + PI3K inhibition may be an effective combination therapy in uveal melanoma, given the inherent reciprocal activation of these pathways within these cells. *Clin Cancer Res; 18(16); 4345–55.* ©*2012 AACR.*

Introduction

Uveal melanoma is the most common intraocular tumor in adults. Approximately half of primary uveal melanoma tumors metastasize. There are no effective therapies for metastatic uveal melanoma, which is fatal in nearly all cases (1). Rational approaches for combination therapy based on activated signal transduction networks may avail new opportunities to effectively treat this disease.

Activating Q209L/P mutations in *GNAQ* and *GNA11* have been identified in approximately 80% of uveal melanoma tumors. *GNAQ* and *GNA11* are very homologous members of the guanine nucleotide-binding G-protein subunit family (2). Under normal conditions, G-proteins are activated by G-protein–coupled receptors and mediate multiple downstream effectors. When mutated on residues R183 or Q209, which disable the intrinsic GTPase enzyme necessary to inhibit G-protein activity, these G-proteins become constitutively activated and oncogenic. To date, there are no direct inhibitors of GNAQ and GNA11.

The mitogen-activated protein/extracellular signal–regulated kinase/mitogen-activated protein kinase (MEK/MAPK) and PI3K/AKT pathways are highly activated in uveal melanoma tumors (3–6). However, uveal melanomas are not observed to harbor activating mutations found in other types of melanoma (e.g., *BRAF*, *NRAS*, or *KIT*) that can

Authors' Affiliations: Departments of [1]Melanoma Medical Oncology, [2]Systems Biology, and [3]Head and Neck Surgery, Ophthalmology Section, University of Texas, MD Anderson Cancer Center, Houston, Texas

Note: Supplementary data for this article are available at Clinical Cancer Research Online (http://clincancerres.aacrjournals.org/).

Corresponding Author: Scott E. Woodman, Melanoma Medical Oncology, MD Anderson Cancer Center, South Campus Research Building, SCR 2.3022, 7455 Fannin St., Houston, TX 77054. Phone: 713-792-2921; Fax: 713-563-3424; E-mail: swoodman@mdanderson.org

doi: 10.1158/1078-0432.CCR-11-3227

Translational Relevance

Uveal melanoma is the most common intraocular tumor in adults. Approximately half of primary uveal melanoma tumors metastasize. Metastatic uveal melanoma is essentially recalcitrant to chemotherapeutic and immunologic therapies and is fatal in nearly all cases. In this study, we show that the combination of clinically relevant mitogen-activated protein/extracellular signal–regulated kinase (MEK) and phosphoinositide 3-kinase (PI3K) small molecule inhibitors potentiates induction of apoptosis in uveal melanoma cells. Importantly, this effect was most pronounced in *GNAQ/11*-mutant cells and not significant in *GNAQ/11* wild-type uveal melanoma cells. These results offer preclinical evidence for the use of combination MEK + PI3K inhibition in metastatic uveal melanoma and suggest that tumors with specific mutations may show variable response to this combination therapy.

stimulate these pathways (7–11). The presence of activating Q209L/P mutations in *GNAQ* or *GNA11* in approximately 80% of uveal melanoma tumors suggests a potential mechanism for the activation of the MEK/MAPK and PI3K/AKT pathways in uveal melanoma (12, 13).

Given the activation of the MEK/MAPK and PI3K/AKT pathways in many cancer types, combination treatment with small molecule inhibitors that target each of these pathways represents a rational therapeutic strategy (14). GSK1120212 is an orally available selective allosteric inhibitor of the MEK1 and MEK2 (MEK1/2) enzymes (15). GSK1120212 has potent *in vitro* and *in vivo* growth-inhibitory effects in cells harboring *RAS* or *BRAF* mutations, for which MEK1/2 is a downstream effector. GSK1120212 has a low C_{max} to C_{trough} ratio and a long half-life, and early phase trials show clinical activity (16). GSK2126458 is an orally available selective inhibitor of the class I phosphoinositide 3-kinase (PI3K) enzymes and MTOR1/2 complexes (17). Biochemical studies show GSK2126458 to have K_i values in the picomolar range for each of the class I PI3K isoforms and MTOR1/2 complexes. GSK2126458 has potent *in vitro* and *in vivo* growth-inhibitory effects on cancer cells. The sustained pharmacodynamic effect at very low circulating drug levels in preclinical models make GSK2126458 a promising clinical therapeutic candidate. Early-phase clinical trials with GSK2126458 are ongoing (ClinicalTrials.gov identifier NCT00972686).

A previous report has shown that exogenous expression of either mutant *GNAQ* or *GNA11* Q209L in immortalized melanocytes injected into the flank of immunodeficient mice results in highly pigmented xenograft lesions (12, 13). In addition, transfection of *GNAQ* or *GNA11* Q209L into melanocytes results in the elevation of MAPK phosphorylation, consistent with the notion that mutant *GNAQ* or *GNA11* activate the MEK/MAPK pathway in uveal melanoma tumors. Like the MEK/MAPK pathway, the PI3K/AKT pathway is highly active in the majority of uveal melanoma tumors, and elevated phosphorylation levels of AKT are associated with a higher risk of metastatic disease (3, 4). However, the effect of activated GNAQ or GNA11 on signaling through the PI3K/AKT pathway seems to be cell-type specific and has not been determined in uveal melanoma (18, 19).

In this study, we use very selective small molecule inhibitors of MEK1/2 and/or PI3K that are currently in multiple clinical trials to inhibit the MEK/MAPK and/or PI3K/AKT pathways in uveal melanoma cell lines with a *GNAQ/11* mutation or wild-type background. We use assays to measure cell growth, cell-cycle regulation, apoptotic induction, and carry out network analysis of proteomic data to determine the relative effects on cellular signaling pathways following treatment with MEK1/2 and PI3K inhibitors, alone and in combination.

Materials and Methods

Cell culture

Cells were cultured in RPMI-1640 supplemented with 5% FBS at 37°C in a humidified 5% CO_2 atmosphere. The MEK inhibitor, GSK1120212 (MEKi), and PI3K inhibitor, GSK2126458 (PI3Ki), were kindly provided by GlaxoSmithKline. siRNAs were purchased from Life Technologies for GNAQ#1 (s5886: UUGUGCAUGAGCCUUAUUGtg), GNAQ#2 (s5887: UCGUCUAUCAUAGCA UUCCtg), GNA11#1 (s5862: AAAGGGUACUCGAUGAUGCcg, GNA11#2 (s5864: UUCUGGUAGACGAGCUUGGtg), BIM#1 (s19474), BIM#2 (s223065), c-JUN#1(s7658), c-JUN#2 (s7659), PLK1 (positive control; s450), and Silencer Select Negative Control No. 1 siRNA (negative control). Oligonucleotides were transfected at 10 nmol/L with Lipofectamine RNAiMax per manufacturer's instructions.

Western blotting

Cells were lysed using radioimmunoprecipitation assay–based lysis buffer supplemented with Na3VO4, phenylmethylsulfonylfluoride, and Protease Cocktail Inhibitors (Invitrogen). Antibodies against GNAQ, GNA11, pMAPK, MAPK1/2, pAKT, AKT, p-cjun, c-jun, glyceraldehyde-3-phosphate dehydrogenase, and PTEN were obtained from Cell Signaling Technology. Antibodies against MAPK2 were obtained from Millipore. Antibodies against BIM were obtained from BioVision.

Reverse phase protein array

The methodologic basis for reverse phase protein array (RPPA) has been previously explicated in detail (20, 21). Cells were treated with MEKi (10 nmol/L) alone, PI3Ki (100 nmol/L) alone, or the combination of MEKi + PI3Ki for 4, 12, or 24 hours. After cellular lysis, protein isolation, quantification, and denaturing, proteins are spotted on nitrocellulose-coated glass slides in serial dilutions. To detect proteins, slides were blocked, then incubated with primary and secondary antibodies and signal amplified by a DakoCytomation catalyzed detection system. Stained slides were scanned, analyzed, and quantitated using Microvigene

software (VigeneTech Inc.) to generate a serial dilution–signal intensity "supercurve" for all samples on the slide. Each sample was then fitted to this "supercurve" to generate logarithmic values representative of relative signal intensity. Differences in protein loading were determined using the median expression level for each sample across all antibodies used; protein values were divided by this factor. Corrected values were used to generate heat maps using Treeview and Xcluster software.

Network analysis

Network analysis was done on the RPPA data to identify reactive signaling networks following treatment with MEKi alone, PI3Ki alone, or both. Data points collected in RPPA experiments were analyzed with Netwalker, as described previously (22, 23). Briefly, protein signal averages were analyzed for the triplicate conditions in ratio (MEKi, PI3Ki, and MEKi + PI3Ki) relative to the untreated cell RPPA signal. For the analysis of proximal alterations in signaling (4 hours) in the *GNAQ*-mutant cell line 92.1, Netwalker analysis was done for each condition, and the top 40 highest interactions based on EF values were composed in a network diagram. Color scale corresponds to the $\log_2$-transformed signal data for the indicated sample comparison. Nodes that were not directly measured in the RPPA analysis were excluded for clarity of presentation. Interacting edges represent protein interactions (PPI).

Cell growth assay

Cells (2.5 E4) were plated in 96-well plates and treated the following day with increasing concentrations of drug or equamolar dimethyl sulfoxide (DMSO) in triplicate. After 72 hours, redox-dye conversion for each treatment was determined using the Cell Titer-Blue Assay (Promega) relative to DMSO alone treatment, by flourometry per the manufacturer's instructions. DMSO vehicle at equimolar concentrations had no significant effect on cell viability in all lines.

Flow cytometry

For cell-cycle analysis, culture supernatants were collected and combined with cultured cells removed by brief trypsin treatment. Cell were washed twice with PBS and fixed with 70% ethanol. Cells were stored overnight at −20°C. Cell were then washed twice with PBS and reconstituted in RNAse A 100 and 20 μg/mL propidium iodide, both purchased from Sigma Aldrich Chemicals and stored at 4°C before analysis. For apoptosis measurements, cells were similarly collected and washed cells were stained with Annexin V, washed once and resuspended in 20 μg/mL propidium iodide. Cells were analyzed on a FACs Canto and data analyzed using FlowJo (Treestar). Cell index was determined as the percent of cells in $S/G_2/M$ phase normalized to untreated baseline cultures. Means of triplicate experiments were compared with repeated measures one-way ANOVA and Bonferroni multiple comparison test using Graphpad prism. Significance indicates a *P* value of less than 0.05 given a confidence interval of 95% of difference.

Spheroids apoptosis assay

Spheroids were generated as previously described (24). Uveal melanoma spheroids were plated in 384-well imaging plates in the presence of the indicated concentrations of MEKi or PI3Ki. Spheroids were treated in triplicate wells and after 44 hours, the CellEvent Caspase-3/7 Green Detection Reagent was added to each well and incubated for 4 hours before imaging. Caspase-active cells were identified as described in manufacturers instruction. Each well was imaged using a BD Biosciences Pathway bioimaging system and analyzed with ImageJ. Drug effect is quantified as caspase-3/7 active cells/spheroid area. Between 4 to 17 spheroids were analyzed per condition.

Results

Effect of GNAQ or GNA11 knockdown on MAPK and AKT signaling and growth in uveal melanoma cells

To examine the dependency on activated mutant *GNAQ* or *GNA11* for growth in uveal melanoma cells that harbor either mutation, siRNAs specific to *GNAQ* or *GNA11* were used. Figure 1A shows the growth-inhibitory effect of *GNAQ* knockdown in uveal melanoma cells with an activating *GNAQ* (Q209L/P) or *GNA11* (Q209L) mutation (hereafter referred to as either *GNAQ* or *GNA11* mutant) or without either a *GNAQ* or *GNA11* mutation (hereafter referred to as "wild type"). siRNA knockdown of *GNAQ* or *GNA11* resulted in a marked inhibition of growth (on par with the siRNA-positive control) in *GNAQ*- or *GNA11*-mutant uveal melanoma cells, respectively, relative to untreated or control (lipid transfectant alone or nontargeting siRNA) treated cells. Neither *GNAQ* nor *GNA11* knockdown in wild-type uveal melanoma cells resulted in a growth-inhibitory effect similar to the siRNA-positive control.

To determine the effect of mutant *GNAQ* or *GNA11* on the MEK/MAPK and PI3K/AKT signaling pathways, Western blot analysis of phosphorylated MAPK (threonine 202, tyrosine 204) and phosphorylated AKT (serine 473) was done following the siRNA knockdown of *GNAQ* or *GNA11* in *GNAQ*- or *GNA11*-mutant uveal melanoma cells, respectively. Figure 1B shows that siRNA knockdown of *GNAQ* or *GNA11* using 2 unique siRNAs in *GNAQ*- or *GNA11*-mutant uveal melanoma cells, respectively, resulted in the loss of MAPK phosphorylation, with no significant change in the phosphorylation of AKT. No significant change in the phosphorylation status of MAPK or AKT was observed after *GNAQ* or *GNA11* knockdown in wild-type uveal melanoma cells. Total levels of MAPK, AKT, or PTEN (a negative regulator of PI3K/AKT signaling) were unchanged after *GNAQ* or *GNA11* knockdown in either *GNAQ*-mutant, *GNA11*-mutant, or wild-type cells. Of note, we have previously shown that the uveal melanoma cell lines used in this study do not harbor genetic alterations previously identified in other types of melanoma (e.g., *NRAS*, *BRAF*, *MEK*, *AKT*, or *PI3K*) that signal through the MEK/MAPK or PI3K/AKT pathways (25).

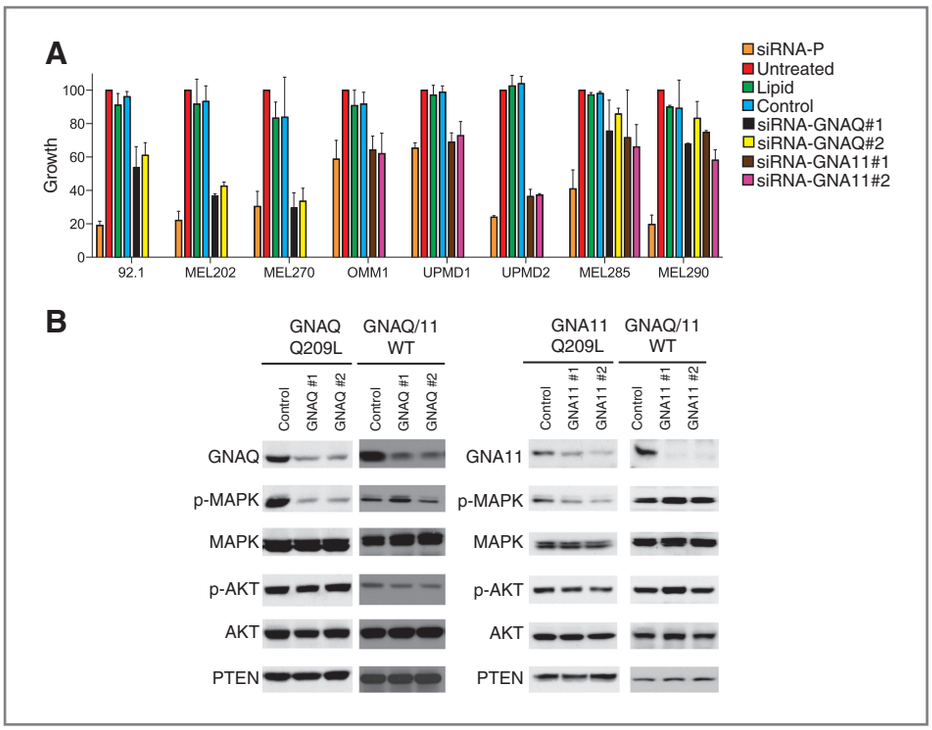

Figure 1. Effect of GNAQ or GNA11 knockdown on cell growth and MAPK/AKT signaling in *GNAQ*-mutant, *GNA11*-mutant, or wild-type uveal melanoma cells. A, *GNAQ*-mutant [Q209L (92.1 and MEL202), Q209P- (MEL 270)] or *GNA11*-mutant [Q209L (OMM1, UPMD1, and UPMD2)], or wild-type (MEL285, MEL290) uveal melanoma cells were transfected with 2 unique siRNAs specific to *GNAQ* or *GNA11*. Cell growth was determined 72 hours after transfection relative to cells that were untreated (untransfected) or transfected with lipid alone, nontargeting siRNA (negative control) or siRNA-targeting PIK1 (positive control, siRNA-P). Combined results of 2 independent experiments; bars, 1 SEM. *B*, Western blot analysis of GNAQ, GNA11, P-MAPK (threonine 202, tyrosine 204), MAPK, P-AKT (serine 473), AKT, and PTEN expression in *GNAQ*-mutant [Q209L (92.1)], *GNA11*-mutant [Q209L (UPMD2)], versus *GNAQ/11* wild-type (MEL285) uveal melanoma cells following transfection with 2 unique *GNAQ* or *GNA11* siRNAs relative to nontargeting control.

Concentration-dependent effect of MEKi or PI3Ki on immediate downstream effectors and uveal melanoma cell growth

All the uveal melanoma cell lines used in this study showed phosphorylation of MAPK and phosphorylation AKT at baseline (Supplementary Fig. S1). Wild-type cell lines showed a greater phospho-MAPK/total MAPK ratio than the GNAQ/11-mutant cell lines. In addition, phospho-AKT levels were moderately less in all the GNA11-mutant cell lines.

Western blot analysis was used to assess the concentration-dependent effect of MEKi (0–1 μmol/L) or PI3Ki (0–1 μmol/L) treatment on the phosphorylation status of their respective downstream effectors, MAPK or AKT. Figure 2A shows that MEKi or PI3Ki treatment of either *GNAQ*-mutant, *GNA11*-mutant, or wild-type cells results in the loss of phosphorylation of their respective downstream targets at low nanomolar concentrations (also see Supplementary Fig. S2). No change in total MAPK or AKT was observed with either treatment in any of the cell lines.

To determine the growth dependency of *GNAQ*- or *GNA11*-mutant or wild-type uveal melanoma cells on activation of the MEK/MAPK or PI3K/AKT pathways, cells were treated with increasing concentrations of either MEKi or PI3Ki. Figure 2B shows *GNAQ*- and *GNA11*-mutant cell growth to be more sensitive to MEKi treatment than wild-type cells, reaching 50% of half-maximal growth inhibition at approximately 1 log less nanomolar concentration. Inversely, wild-type cells reached 50% of half-maximal growth at lower PI3Ki concentrations.

Given the limitations inherent in redox dye assays to assess growth inhibition, real-time impedance measurements were also carried out. Cell impedance is affected by 3 factors: cell growth, cell spreading, and loss of attachment. Impedance measurements were taken over time in *GNAQ*-mutant and wild-type cells with increasing concentrations of MEKi (0–500 nmol/L) or PI3Ki (0–1,000 nmol/L) compared with no treatment (Supplementary Fig. S3). MEKi treatment resulted in an initial inflection in impedance that corresponded with the morphologic spreading of the cell lines. However, a marked concentration-dependent reduction in impedance in *GNAQ*-mutant cells was observed over time, which was not observed in wild-type cells. PI3Ki treatment resulted in a similar reduction in impedance in both *GNAQ*-mutant and wild-type cells. A differential loss of cells from the plate surface was not observed in either mutant or wild-type cells.

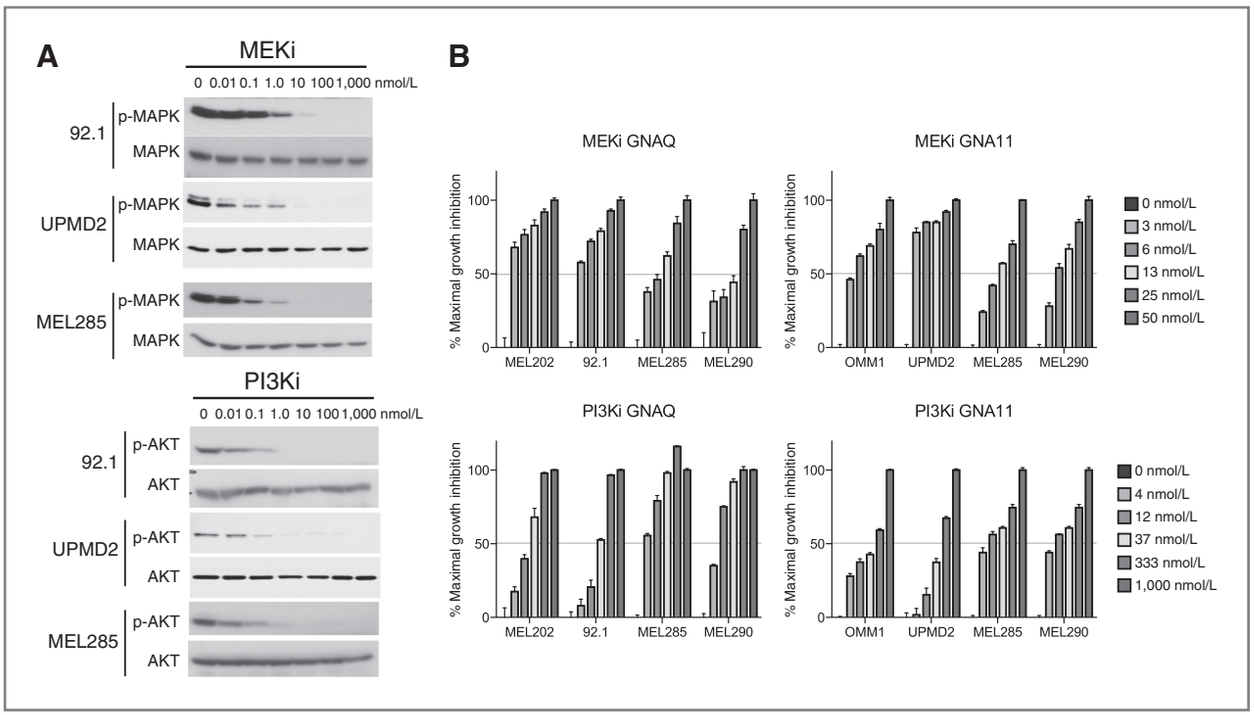

Figure 2. Effect of small molecule MEK or PI3K inhibitors on *GNAQ*-mutant, *GNA11*-mutant, or wild-type uveal melanoma cell growth and MAPK/AKT signaling. *GNAQ*-mutant [Q209L (92.1, MEL202)] or *GNA11*-mutant [Q209L (OMM1, UPMD2)], or *GNAQ/11* wild-type (MEL285, MEL 290) uveal melanoma cells were used for the following experiments: A, uveal melanoma cells were treated with increasing doses of GSK1120212 (MEK inhibitor, MEKi) or GSK2126458 (PI3K inhibitor, PI3Ki) for 3 hours and expression of P-MAPK, MAPK, P-AKT, and AKT determined by Western blot analysis. B, uveal melanoma cells were treated with increasing doses of MEKi or PI3Ki for 72 hours and percent of maximal cell growth inhibition determined (representative experiments; bars, SD).

Effect of MEKi and/or PI3Ki treatment on MAPK and AKT signaling pathways, cell cycle and apoptosis mediators in uveal melanoma cells

RPPA was used to assess the effect of MEKi alone, PI3Ki alone, or combination MEKi + PI3Ki treatment on the MEK/MAPK and PI3K/AKT signaling pathways, the Rb cell-cycle regulator, and apoptosis mediators in uveal melanoma cells.

Figure 3A shows that both mutant and wild-type uveal melanoma cells show a marked reduction in MAPK phosphorylation after MEKi treatment. PI3Ki treatment resulted in the reduction of phosphorylation in AKT, notably in *GNAQ* wild-type cells. A reciprocal increase in AKT phosphorylation after MEKi treatment and an increase MAPK phosphorylation after PI3Ki treatment was also noted. However, these effects seemed dependent on the relative expression of phosphorylated MAPK or AKT at baseline. If MAPK or AKT phosphorylation levels were relatively high at baseline, a drug-induced increase was not observed. Combination MEKi + PI3Ki treatment resulted in a decrease in phosphorylation in both MAPK and AKT in both *GNAQ*-mutant and wild-type cells without a reciprocal increase in AKT or MAPK phosphorylation, respectively.

MEKi alone treatment resulted in the relative decrease in phosphorylation of p70S6K (threonine 389), with little change in 4EBP1 (serine 65, threonine 37) or S6 phosphorylation (serine 236/244) in *GNAQ*-mutant and wild-type cells. PI3Ki alone treatment resulted in decreased phosphorylation of 4EBP1, S6, and p70S6K in *GNAQ*-mutant and wild-type cells, although the complete extinguishment of S6 phosphorylation required combination MEKi + PI3Ki treatment in mutant cells.

MEKi alone treatment resulted in a stark reduction in myc transcription factor levels after 12 hours with a corresponding reduction in the phosphorylation of Rb (serine 807/811) in *GNAQ*-mutant cells. PI3Ki alone treatment resulted in decreased Rb phosphorylation in both *GNAQ*-mutant and wild-type cells, but failed to have any effect on myc levels. Combination MEKi + PI3Ki treatment resulted in no greater reductions in myc or Rb phosphorylation than MEKi treatment alone.

Molecular mediators of apoptosis were assessed after 24 hours of MEKi alone, PI3Ki alone, or MEKi + PI3Ki combination treatment. Neither MEKi nor PI3Ki treatment alone resulted in significant elevation in cleaved caspase-3 or caspase-7 in mutant or wild-type cells. However, combination MEKi + PI3Ki treatment resulted in a marked increase in cleaved caspase-3 and caspase-7 levels in *GNAQ*-mutant cells, not observed in wild-type cells. No clear trend in Bcl-2 family member protein expression was observed after MEKi and/or PI3Ki treatment in any of the cell lines, with the exception of BIM, which was elevated after MEKi

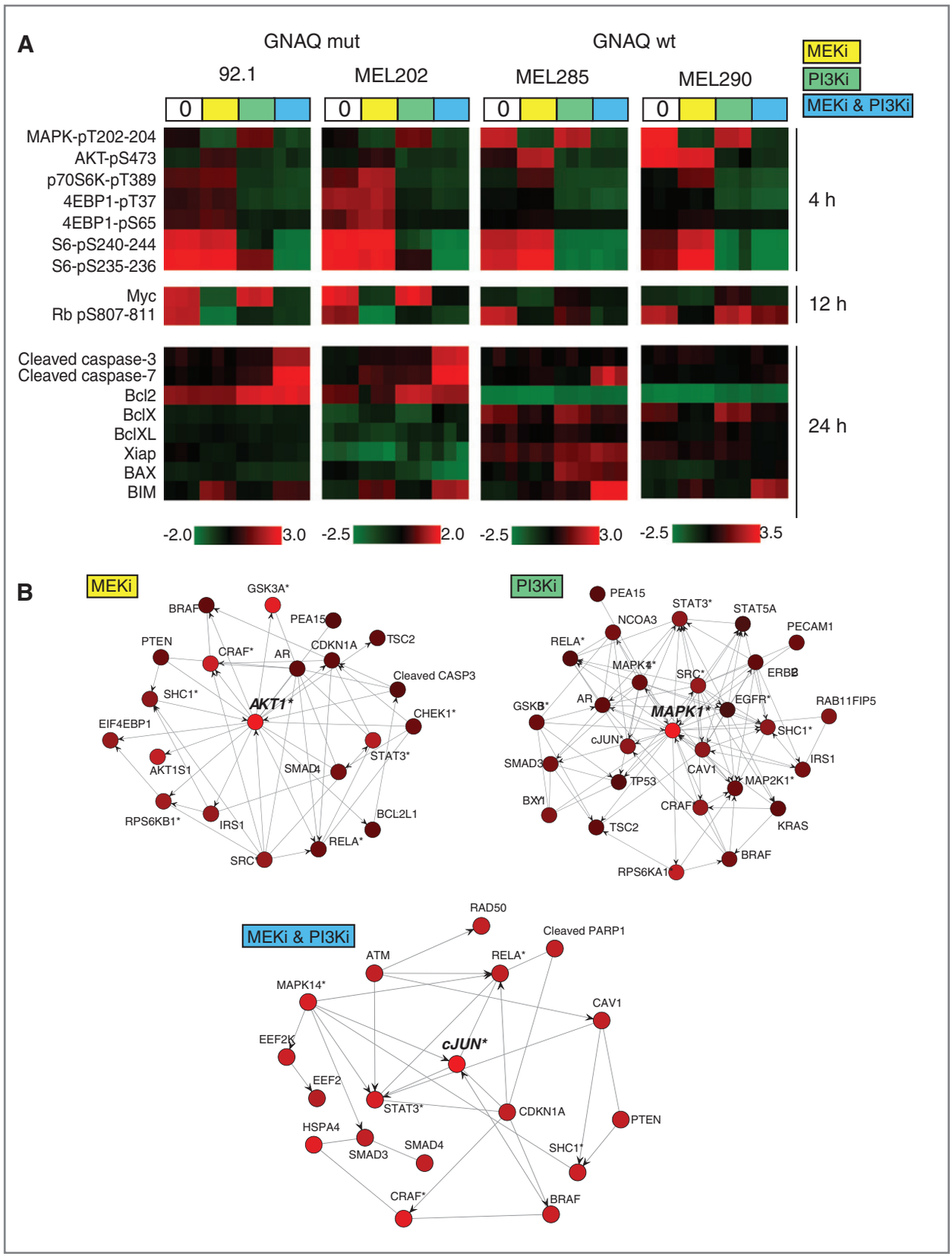

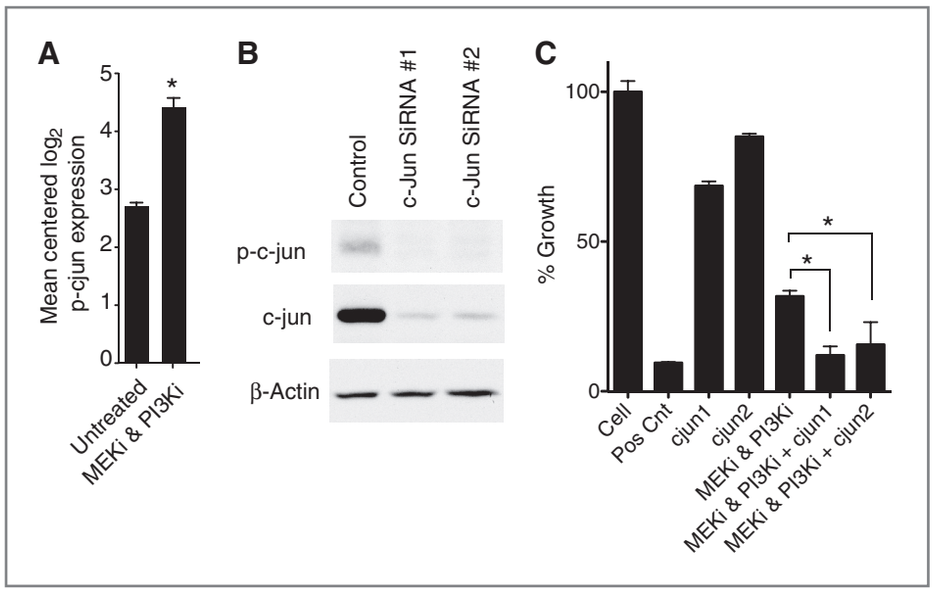

Figure 4. Effect of c-jun knockdown on combination MEKi + PI3Ki treatment of uveal melanoma cells. A, GNAQ Q209L-mutant uveal melanoma cells (92.1) were treated with combination MEKi (10 nmol/L) + PI3Ki (100 nmol/L) for 4 hours and levels of phosphorylated c-jun determined relative to untreated cells. B, cells were transfected with 2 distinct siRNAs targeting c-jun, then levels of phosphorylated c-jun, total c-jun, or β-actin were determined by Western blot. C, cells were transfected with -2 distinct siRNAs targeting c-jun, then treated with combination MEKi (10 nmol/L) + PI3Ki (100 nmol/L). The effect of c-jun knockdown in MEKi + PI3Ki treated cells was compared with the effect of MEKi + PI3Ki treatment alone. *, $P < 0.05$.

alone and combination MEKi + PI3Ki treatment in both mutant and wild-type cells.

To determine whether elevated levels of BIM following MEKi + PI3Ki treatment mediated cleavage of caspase-3 and caspase-7 in *GNAQ*-mutant cells, 2 distinct siRNAs targeting BIM were used. Cells were transfected with BIM siRNAs, then treated with MEKi + PI3Ki. Targeting BIM was unable to rescue the apoptotic effect of MEKi + PI3Ki treatment (Supplementary Fig. S4).

To characterize the nature of signaling molecule interactions induced by MEKi alone, PI3Ki alone, or combination MEKi + PI3Ki treatment, network-based analysis was done on the *GNAQ* (Q209L)-mutant cell line 92.1. NetWalk is a random walk–based algorithm that scores the relevance of protein–protein interactions (represented as "edge flux" values) based on protein expression level values in the context of neighboring nodes (proteins) and local network connectivity. Figure 3B shows the highest scoring networks following MEKi alone, PI3Ki alone, or combination MEKi + PI3Ki treatment compared with no treatment. Following MEKi alone treatment, among the highest scoring interactants within the signaling network was AKT phosphorylated on serine 473. Conversely, network analysis following PI3Ki alone treatment showed phosphorylated MAPK (threonine 202, tyrosine 204) to be among the highest scoring interactants within the signaling network. Combination MEKi + PI3Ki treatment revealed a distinct signaling network pattern in which neither phosphorylated MAPK nor AKT were relevant; rather, the transcription factor c-jun (pS73) became central to the network with multiple interactions with other signaling molecules [e.g., JNK, STAT3, NfκB (RelA)]. Similar data was observed with the *GNAQ*-mutant MEL 202 (not shown).

Given the central role of phosphorylated c-jun (p-cjun) indicated by network analysis following combination MEKi + PI3Ki treatment, protein levels of p-cjun at baseline and following MEKi + PI3Ki treatment was evaluated. The p-cjun protein showed a significant increase following combination MEKi + PI3Ki treatment (Fig. 4A and Supplementary Fig. S5). To gain greater insight into the potential functional implication of elevated p-cjun in this context, 2 distinct siRNAs targeting p-cjun were used. Figure 4B shows a marked loss of c-jun and p-cjun expression following siRNA knockdown of c-jun. A growth assay shows knockdown of c-jun to have a modest effect on uveal melanoma cell growth at baseline; however, knockdown of c-jun significantly enhanced the growth-inhibitory effect of MEKi + PI3Ki treatment (Fig. 4C).

Effect of MEKi and/or PI3Ki treatment on cell-cycle regulation in uveal melanoma cells

To determine the effect of MEKi and/or PI3Ki treatment on cell-cycle regulation in uveal melanoma cells at the single

Figure 3. Effect of small molecule MEK and/or PI3K inhibitors on signaling pathways in *GNAQ*-mutant versus wild-type uveal melanoma. A, mutant *GNAQ* [Q209L (92.1, MEL202)] or wild-type (MEL285, MEL290) uveal melanoma cells were treated with MEKi alone (10 nmol/L), PI3Ki alone (100 nmol/L), or the combination of MEKi + PI3Ki for 4, 12, or 24 hours. RPPA was carried out to assess the expression of proteins in the MEK/MAPK, PI3K/AKT, cell-cycle, and apoptosis pathways. The heat map represents the mean centered $\log_2$ expression value for each protein after the indicated time of treatment (red, greater; green, lesser). Each treatment was carried out in triplicate; therefore there are 3 distinct heat map boxes per treatment condition. B, the highest scoring network interactions (edge flux values) from the NetWalk analysis of directly measured proteins following 4 hours of MEKi and/or PI3Ki treatment. Nodes represent proteins, edges represent network interactions among nodes, node coloring represents relative increase in protein level. Asterisks (*) indicate phosphorylated proteins.

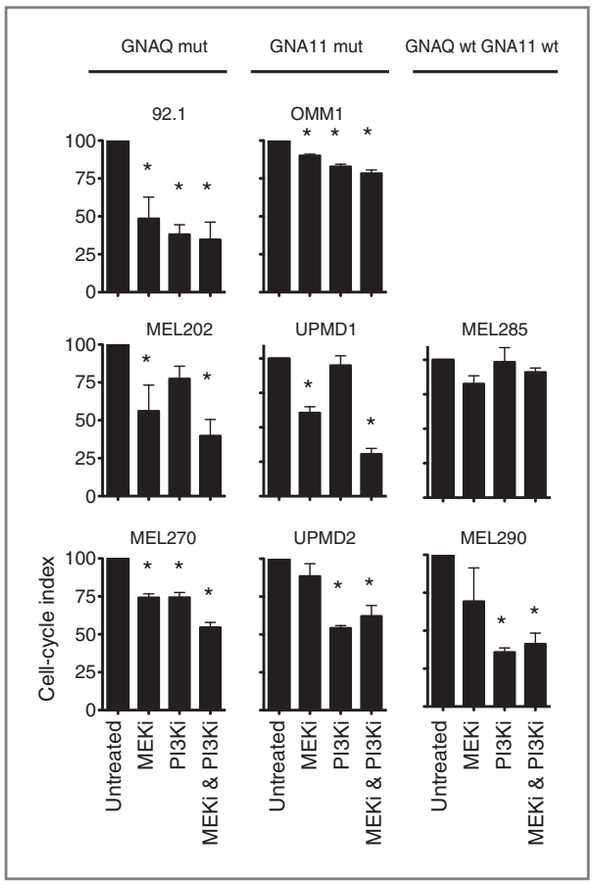

Figure 5. Effect of small molecule MEK and/or PI3K inhibitors on cell-cycle regulation in *GNAQ*-mutant, *GNA11*-mutant, or wild-type uveal melanoma cells. The indicated mutant *GNAQ*, mutant *GNA11*, or wild-type uveal melanoma cells were treated with MEKi alone, PI3Ki alone, or the combination of MEKi + PI3Ki for 24 hours. Cell-cycle regulation was assessed by single-cell flow cytometry analysis and the percent of cells in the $S/G_2/M$ phases determined. Cell index was determined as the percent of cells in $S/G_2/M$ phase normalized to untreated baseline cultures; bars, 1 SEM. Means of triplicate experiments were compared with repeated measures one-way ANOVA and Bonferroni multiple comparison test using Graphpad prism. Significance indicates a *P* value less than 0.05 given a confidence interval of 95% of difference.

cell level, we carried out flow cytometric analysis of DNA content in *GNAQ*-mutant, *GNA11*-mutant, or wild-type cells treated with MEKi alone, PI3Ki alone, or the combination. The percent of cells in the $S/G_2/M$ phases was determined relative to untreated cells (Fig. 5). MEKi treatment resulted in a significant decrease in cycling cells in the majority of uveal melanoma cell lines (3 of 3 *GNAQ* mutant, 2 of 3 *GNA11* mutant, and 0 of 2 wild type). Similarly, uveal melanoma cell lines showed a significant decrease in cycling cells after PI3Ki treatment alone (2 of 3 *GNAQ* mutant, 2 of 3 *GNA11* mutant, and 1 of 2 wild type). The combination of MEKi + PI3Ki treatment further decreased the number of cycling cells in the majority of cell lines compared with MEKi or PI3Ki alone treatment (3 of 3 *GNAQ* mutant, 3 of 3 *GNA11* mutant, and 1 of 2 wild type).

Effect of MEKi and/or PI3Ki treatment on apoptosis induction in uveal melanoma cells

To examine the capacity of MEKi and/or PI3Ki treatment to induce apoptosis in uveal melanoma cells, flow cytometry assessment of Annexin V and propidium iodide staining was done. Analysis of the induction of apoptosis over 3 days in response to treatment with MEKi alone, PI3Ki alone, or the combination of MEKi + PI3Ki indicated that the 48-hour response allows for the reliable detection of early apoptotic cells. After 72 hours of treatment with the combination of MEKi + PI3Ki, few cells are available to assay in drug-sensitive lines as shown in Fig. 6A.

GNAQ-mutant, *GNA11*-mutant, or wild-type cells were treated with MEKi alone, PI3Ki alone, or the combination of MEKi + PI3Ki. Figure 6B shows MEKi treatment alone resulted in little to no induction of early apoptosis in all the uveal melanoma cell lines tested, with the exception of the *GNAQ*-mutant MEL270 cell lines, in which 55% of cells (relative to baseline) were observed to have an early apoptotic response. PI3Ki alone treatment also resulted in a modest induction of early apoptosis in all the uveal melanoma cell lines tested, with the exception of the *GNAQ*-mutant MEL 270 cell line (38%, relative to baseline). A clearer mutant genotype-dependent apoptotic response was observed with MEKi + PI3Ki combination treatment. *GNAQ*-mutant cells showed a marked induction of early apoptosis after MEKi + PI3Ki combination treatment (70% in MEL270, 55% in 92.1, and 44% in MEL202). *GNA11*-mutant and wild-type cells displayed a variable apoptotic response to MEKi + PI3Ki combination treatment (*GNA11* = 20% in UPMD2, 20% in OMM1, and 4% in UPMD1; wild-type = 5% in MEL285 and 7% in MEL290).

Prior studies have shown that drug treatments that show efficacy in 2-dimensional cultures can fail when cells are grown in 3-dimensional (3D) tumor-like structures (26). Thus, to examine the effect of MEKi + PI3Ki treatment in a 3D cellular system, we generated uveal melanoma cell spheroids (Fig. 6C). Spheroids were treated with MEKi (0, 3.1, or 12.5 nmol/L) and/or PI3Ki (0, 6.25, or 100 nmol/L) and assessed for caspase-3/7 activity using a fluorescent substrate reporter by high-throughput confocal microscopy (Fig. 6D). The cells making up spheroids showed negligible caspase-3/7 activity at baseline. Increasing doses of either MEKi or PI3Ki resulted in a modest increase in caspase-3/7 activity within spheroid cells (Fig. 6E). However, combination of MEKi + PI3Ki treatment resulted in markedly elevated caspase-3/7 activity within spheroid cells. Single cells that were unincorporated into spheroids tended to show caspase-3/7 activity under all treatment conditions.

Discussion

Functional studies in uveal melanoma research have been hampered by the paucity of cell lines available for analysis. Of cell lines noted to be of uveal origin, many have been identified to have an activating V600E mutation in *BRAF*, despite *BRAF* mutations not being identified in uveal

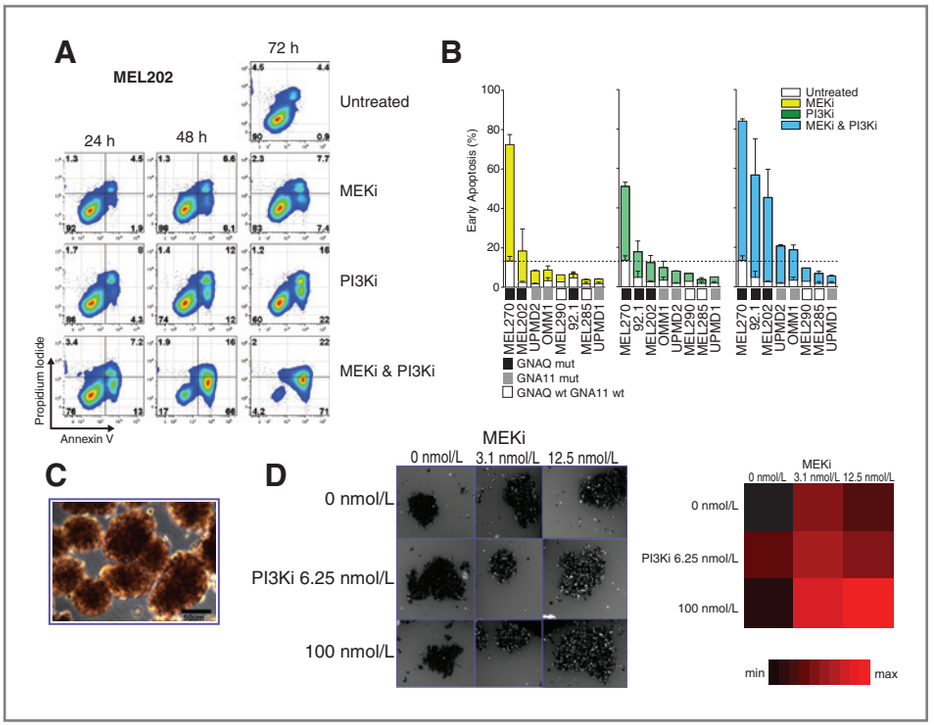

Figure 6. Effect of small molecule MEK and/or PI3K inhibitors on apoptosis induction in *GNAQ*-mutant, *GNA11*-mutant, or wild-type uveal melanoma cells. A, representative flow cytometry experiment assessing levels of Annexin V and propidium iodide in *GNAQ*-mutant cells (MEL202) after MEKi alone, PI3Ki alone, or the combination of MEKi + PI3Ki treatment at 24, 48, and 72 hours. B, mutant *GNAQ* [Q209L (92.1, MEL202), Q209P (MEL270)], mutant *GNA11* [Q209L (OMM1, UPMD1, UPMD2)], or wild-type (MEL285, MEL290) uveal melanoma cells were treated with MEKi alone, PI3Ki alone, or the combination of MEKi + PI3Ki for 48 hours. Induction of apoptosis was assessed by flow cytometry using Annexin V and propidium iodide staining. The percent of cells in early apoptosis was determined by gating the high Annexin V/low propidium iodide cell population following treatment. Data represents $n = 3$–6 experiments; bars, 1 SEM. C, light microscopy image of uveal melanoma spheroids (bar, 50 um). D, confocal microscopic imaging of caspase-3/7 activity in cells within uveal melanoma spheroids (UPMD2) following treatment with increasing doses of MEKi and/or PI3Ki. Heat map represents caspase-3/7–positive cells per spheroid area.

melanoma tissues using standard techniques (5, 8–10, 27, 28). Given that approximately 80% of uveal melanoma tumors harbor mutually exclusive *Q209* mutations in *GNAQ* or *GNA11*, use of uveal melanoma cell lines with these mutations are a powerful tool to assess the efficacy of targeted therapeutic approaches. This study uses the largest number of *GNAQ*-mutant, *GNA11*-mutant, or wild-type uveal melanoma cell lines to date to determine the relative efficacy of using very selective MEK and/or PI3K inhibitors in uveal melanoma.

Activation of the MEK/MAPK and PI3K/AKT pathways in all types of melanoma, including uveal melanoma tumors, has been extensively documented (3, 4, 6, 29). Activating mutations in *BRAF*, *NRAS*, *KIT*, *AKT*, *PI3K*, and loss of PTEN are mechanisms by which the MEK/MAPK and PI3K/AKT pathways are activated in cutaneous melanoma. We have previously determined that the uveal melanoma cell lines examined in this study lack common mutations in *BRAF*, *NRAS*, *KIT*, *AKT*, *PI3K*, or loss of PTEN and consistent with their uveal melanoma tissue counterparts, harbor mutually exclusive activating Q209L/P mutations in *GNAQ* or *GNA11* (25). Activated GNAQ/11 have been proposed to be both activators and inhibitors of the MEK/MAPK and PI3K/AKT pathways in different biochemical and noncancer cell studies (18, 19). Thus we investigated the relative contribution of mutation-activated GNAQ or GNA11 on MEK/MAPK and/or PI3K/AKT signaling in uveal melanoma cells. Knockdown of *GNAQ* or *GNA11* resulted in diminished MAPK phosphorylation in uveal melanoma cell lines with *GNAQ* or *GNA11* mutations, respectively, but not in wild-type cells, confirming that activated GNAQ or GNA11 signal through the MEK/MAPK pathway in *GNAQ- or GNA11*-mutant uveal melanoma, respectively. However, loss of mutant *GNAQ* or *GNA11* had no significant effect on AKT phosphorylation in either *GNAQ*- or *GNA11*-mutant or wild-type uveal melanoma cell lines. We show that inhibition of MEK and, therefore, MAPK signaling results in the reciprocal activation of AKT activity in uveal melanoma cell lines, regardless of *GNAQ/11*-mutant status.

It has been proposed that tumors with activating mutations in the RAS/RAF axis depend more on MAPK signaling, whereas activating mutations in receptor tyrosine kinases depend more on PI3K signaling (30). Data presented in this article suggest that the activating mutations in *GNAQ* and *GNA11* are akin to mutations in the RAS/RAF axis, given their greater sensitivity to growth inhibition following treatment with a selective MEKi and loss of MAPK phosphorylation with *GNAQ or GNA11* loss, respectively. This

conclusion is further supported by previous data that shows 4EBP1 to be a redundant downstream mediator in tumors with coexistent mutational activation of the MEK/MAPK and PI3K/AKT pathways (e.g., colon carcinomas with both *KRAS* and *PI3KCA* mutations; ref. 31). The mutant uveal melanoma cells examined in this study showed marked loss of 4EBP1 phosphorylation only after PI3Ki treatment, with no significant additional loss with combination MEKi + PI3Ki treatment. The fact that the PI3Ki treatment effects on cell growth, cell-cycle regulation, and apoptosis induction were similar in all uveal melanoma cells tested, which suggests that non-*GNAQ/11* mutant–driven mechanisms may drive the PI3K/AKT pathway in uveal melanoma.

Given the clear activation of the MEK/MAPK pathway by mutant *GNAQ* or *GNA11*, inhibition of MEK would seem to be a rational therapeutic approach in patients with *GNAQ- or GNA11*-mutant tumors. In a phase I clinical trial, Adjeiand colleagues reported one patient with both metastatic uveal melanoma and renal cell carcinoma to have stable disease for 22 cycles on the AZD6244 MEK inhibitor (32). A review of 3 completed trials in which 20 patients with metastatic uveal melanoma were treated either upfront with AZD6244 or following progression on temozolomide suggested an improvement in progression-free survival in favor of MEK inhibitor treatment, although too few patients were treated to definitively make this conclusion (33). Finally, a phase I clinical trial has recently been completed, which used the GSK1120212 MEK inhibitor. Seventy-two melanoma patients, including uveal melanoma patients, were enrolled, but the outcomes have yet to be published (22). None of the aforementioned studies systematically evaluated the *GNAQ* or *GNA11* mutation status of tumors to determine whether efficacy correlated with *GNAQ* mutation, *GNA11* mutation, or wild-type status. A clinical trial powered to determine the efficacy of MEK inhibition in *GNAQ/11*-mutant uveal melanoma is ongoing (23).

Data presented in this article suggests that MEK inhibition alone is able to achieve cell-cycle arrest and reduce growth in most uveal melanoma cells, but only results in modest apoptotic cell death in the majority of uveal melanoma cells. Likewise, PI3K inhibition alone can cause cell-cycle arrest and reduced growth but is insufficient to induce substantive apoptotic death. However, the combination of MEK + PI3K inhibition results in a strong induction of apoptotic death, most pronounced in *GNAQ*-mutant cells and also evident in the majority of *GNA11*-mutant cells. Proteomic network analysis reveals a homeostatic relationship between the MEK/MAPK and PI3K/AKT pathways in uveal melanoma cells—inhibition of MEK resulted in a relative increase in AKT phosphorylation, whereas an increase in the phosphorylation of MAPK was elicited after inhibition of PI3K. Similar feedback regulatory mechanisms have been observed in cancers driven by activating *RAS* or *RAF* mutations in lung, breast, and cutaneous melanoma (34–36). In addition, signaling network analysis of proteomic data revealed that inhibition of both the MEK/MAPK and PI3K/AKT pathways increases the activation of the transcription factor c-jun. Knockdown of c-jun significantly enhanced the growth-inhibitory effects of combination MEKi + PI3Ki therapy, suggesting that c-jun may play a potential compensatory role in cell growth after treatment.

The preclinical data presented in this article support the MEK/MAPK pathway as an important effector of *GNAQ/11*-mutant signaling and MEK inhibition as a therapeutic strategy to mitigate cell growth. Combinatorial targeted therapies, such as the one used in this study, using MEK inhibitors as a "back-bone" may offer greater therapeutic effect by enhancing uveal melanoma cell death.

Disclosure of Potential Conflicts of Interest

S.E. Woodman and M.A. Davies have both received research funding from GlaxoSmithKline. GSK1120212 and GSK2126458, compounds used in this study, are from GlaxoSmithKline.

Grant Support

S.E. Woodman is a recipient of the NCI Melanoma SPORE Career Development Program Award (P50CA093459) and the NIH Paul Calabresi Clinical Oncology Award (K12CA088084). The work was supported by GlaxoSmithKline research grant (S.E. Woodman and M.A. Davies), flow cytometry CCSG core grant 5P30CA0166712, and NCI # CA16672 for RPPA Development and services.

The costs of publication of this article were defrayed in part by the payment of page charges. This article must therefore be hereby marked *advertisement* in accordance with 18 U.S.C. Section 1734 solely to indicate this fact.

Received December 14, 2011; revised May 30, 2012; accepted June 1, 2012; published OnlineFirst June 25, 2012.

References

1. Bedikian AY. Metastatic uveal melanoma therapy: current options. Int Ophthalmol Clin 2006;46:151–66.
2. Kimple AJ, Bosch DE, Giguere PM, Siderovski DP. Regulators of G-protein signaling and their Galpha substrates: promises and challenges in their use as drug discovery targets. Pharmacol Rev 2011;63:728–49.
3. Populo H, Soares P, Rocha AS, Silva P, Lopes JM. Evaluation of the mTOR pathway in ocular (uvea and conjunctiva) melanoma. Melanoma Res 2010;20:107–17.
4. Saraiva VS, Caissie AL, Segal L, Edelstein C, Burnier MN Jr. Immunohistochemical expression of phospho-Akt in uveal melanoma. Melanoma Res 2005;15:245–50.
5. Weber A, Hengge UR, Urbanik D, Markwart A, Mirmohammadsaegh A, Reichel MB, et al. Absence of mutations of the BRAF gene and constitutive activation of extracellular-regulated kinase in malignant melanomas of the uvea. Lab Invest 2003;83:1771–6.
6. Zuidervaart W, van Nieuwpoort F, Stark M, Dijkman R, Packer L, Borgstein AM, et al. Activation of the MAPK pathway is a common event in uveal melanomas although it rarely occurs through mutation of BRAF or RAS. Br J Cancer 2005;92:2032–8.
7. All-Ericsson C, Girnita L, Muller-Brunotte A, Brodin B, Seregard S, Ostman A, et al. c-Kit-dependent growth of uveal melanoma cells: a potential therapeutic target? Invest Ophthalmol Vis Sci 2004;45:2075–82.
8. Cohen Y, Goldenberg-Cohen N, Parrella P, Chowers I, Merbs SL, Pe'er J, et al. Lack of BRAF mutation in primary uveal melanoma. Invest Ophthalmol Vis Sci 2003;44:2876–8.
9. Cruz F 3rd, Rubin BP, Wilson D, Town A, Schroeder A, Haley A, et al. Absence of BRAF and NRAS mutations in uveal melanoma. Cancer Res 2003;63:5761–6.
10. Edmunds SC, Cree IA, Di Nicolantonio F, Hungerford JL, Hurren JS, Kelsell DP. Absence of BRAF gene mutations in uveal

melanomas in contrast to cutaneous melanomas. Br J Cancer 2003;88:1403–5.
11. Pache M, Glatz K, Bosch D, Dirnhofer S, Mirlacher M, Simon R, et al. Sequence analysis and high-throughput immunohistochemical profiling of KIT (CD 117) expression in uveal melanoma using tissue microarrays. Virchows Arch 2003;443:741–4.
12. Van Raamsdonk CD, Bezrookove V, Green G, Bauer J, Gaugler L, O'Brien JM, et al. Frequent somatic mutations of GNAQ in uveal melanoma and blue naevi. Nature 2009;457:599–602.
13. Van Raamsdonk CD, Griewank KG, Crosby MB, Garrido MC, Vemula S, Wiesner T, et al. Mutations in GNA11 in uveal melanoma. N Engl J Med 2010;363:2191–9.
14. Jiang X, Zhou J, Yuen NK, Corless CL, Heinrich MC, Fletcher JA, et al. Imatinib targeting of KIT-mutant oncoprotein in melanoma. Clin Cancer Res 2008;14:7726–32.
15. Gilmartin AG, Bleam MR, Groy A, Moss KG, Minthorn EA, Kulkarni SG, et al. GSK1120212 (JTP-74057) is an inhibitor of MEK activity and activation with favorable pharmacokinetic properties for sustained *in vivo* pathway inhibition. Clin Cancer Res 2011;17: 989–1000.
16. Infante JR, Fecher LA, Nallapareddy S, Gordon MS, Flaherty KT, Cox DJ, et al. Safety and efficacy results from the first-in-human study of the oral MEK 1/2 inhibitor GSK1120212. J Clin Oncol 2010;28:15S–S.
17. Steven D Knight NDA, Burgess Joelle L, Chaudhari Amita M, Darcy Michael G, Donatelli Carla A, Luengo Juan I, et al. Discovery of GSK2126458, a highly potent inhibitor of PI3K and the mammalian target of rapamycin. ACS Med Chem Lett 2010;1:39–43.
18. Ballou LM, Chattopadhyay M, Li Y, Scarlata S, Lin RZ. Galphaq binds to p110alpha/p85alpha phosphoinositide 3-kinase and displaces Ras. Biochem J 2006;394:557–62.
19. Howes AL, Miyamoto S, Adams JW, Woodcock EA, Brown JH. Galphaq expression activates EGFR and induces Akt mediated cardiomyocyte survival: dissociation from Galphaq mediated hypertrophy. J Mol Cell Cardiol 2006;40:597–604.
20. Hennessy BT, Lu Y, Poradosu E, Yu Q, Yu S, Hall H, et al. Pharmacodynamic markers of perifosine efficacy. Clin Cancer Res 2007;13: 7421–31.
21. Tibes R, Qiu Y, Lu Y, Hennessy B, Andreeff M, Mills GB, et al. Reverse phase protein array: validation of a novel proteomic technology and utility for analysis of primary leukemia specimens and hematopoietic stem cells. Mol Cancer Ther 2006;5:2512–21.
22. Lu Y, Muller M, Smith D, Dutta B, Komurov K, Iadevaia S, et al. Kinome siRNA-phosphoproteomic screen identifies networks regulating AKT signaling. Oncogene 2011;30:4567–77.
23. Komurov K, White MA, Ram PT. Use of data-biased random walks on graphs for the retrieval of context-specific networks from genomic data. PLoS Comput Biol 2010;6.
24. Li AP, Colburn SM, Beck DJ. A simplified method for the culturing of primary adult rat and human hepatocytes as multicellular spheroids. In Vitro Cell Dev Biol 1992;28A:673–7.
25. Griewank KG, Yu X, Khalili J, Sozen MM, Stempke-Hale K, Bernatchez C, et al. Genetic and molecular characterization of uveal melanoma cell lines. Pigment Cell Melanoma Res 2012;25:182–7.
26. Smalley KS, Haass NK, Brafford PA, Lioni M, Flaherty KT, Herlyn M. Multiple signaling pathways must be targeted to overcome drug resistance in cell lines derived from melanoma metastases. Mol Cancer Ther 2006;5:1136–44.
27. Janssen CS, Sibbett R, Henriquez FL, McKay IC, Kemp EG, Roberts F. The T1799A point mutation is present in posterior uveal melanoma. Br J Cancer 2008;99:1673–7.
28. Maat W, Kilic E, Luyten GP, de Klein A, Jager MJ, Gruis NA, et al. Pyrophosphorolysis detects B-RAF mutations in primary uveal melanoma. Invest Ophthalmol Vis Sci 2008;49:23–7.
29. Meier F, Schittek B, Busch S, Garbe C, Smalley K, Satyamoorthy K, et al. The RAS/RAF/MEK/ERK and PI3K/AKT signaling pathways present molecular targets for the effective treatment of advanced melanoma. Front Biosci 2005;10:2986–3001.
30. Sos ML, Fischer S, Ullrich R, Peifer M, Heuckmann JM, Koker M, et al. Identifying genotype-dependent efficacy of single and combined PI3K- and MAPK-pathway inhibition in cancer. Proc Natl Acad Sci U S A 2009;106:18351–6.
31. She QB, Halilovic E, Ye Q, Zhen W, Shirasawa S, Sasazuki T, et al. 4E-BP1 is a key effector of the oncogenic activation of the AKT and ERK signaling pathways that integrates their function in tumors. Cancer Cell 2010;18:39–51.
32. Adjei AA, Cohen RB, Franklin W, Morris C, Wilson D, Molina JR, et al. Phase I pharmacokinetic and pharmacodynamic study of the oral, small-molecule mitogen-activated protein kinase kinase 1/2 inhibitor AZD6244 (ARRY-142886) in patients with advanced cancers. J Clin Oncol 2008;26:2139–46.
33. Patel M, Smyth E, Chapman PB, Wolchok JD, Schwartz GK, Abramson DH, et al. Therapeutic implications of the emerging molecular biology of uveal melanoma. Clin Cancer Res 2011;17:2087–100.
34. Engelman JA, Chen L, Tan X, Crosby K, Guimaraes AR, Upadhyay R, et al. Effective use of PI3K and MEK inhibitors to treat mutant Kras G12D and PIK3CA H1047R murine lung cancers. Nat Med 2008;14: 1351–6.
35. Hoeflich KP, O'Brien C, Boyd Z, Cavet G, Guerrero S, Jung K, et al. *In vivo* antitumor activity of MEK and phosphatidylinositol 3-kinase inhibitors in basal-like breast cancer models. Clin Cancer Res 2009;15: 4649–64.
36. Gopal YN, Deng W, Woodman SE, Komurov K, Ram P, Smith PD, et al. Basal and treatment-induced activation of AKT mediates resistance to cell death by AZD6244 (ARRY-142886) in Braf-mutant human cutaneous melanoma cells. Cancer Res 2010;70:8736–47.